
This is an electronic reprint of the original article.
This reprint may differ from the original in pagination and typographic detail.

Kim, D.-H.; Törmä, P.

Fulde-Ferrell-Larkin-Ovchinnikov state in the dimensional crossover between one- and three-dimensional lattices

Published in:
Physical Review B

DOI:
[10.1103/PhysRevB.85.180508](https://doi.org/10.1103/PhysRevB.85.180508)

Published: 01/01/2012

Document Version
Publisher's PDF, also known as Version of record

Please cite the original version:
Kim, D.-H., & Törmä, P. (2012). Fulde-Ferrell-Larkin-Ovchinnikov state in the dimensional crossover between one- and three-dimensional lattices. *Physical Review B*, 85(18), 1-4. [180508].
<https://doi.org/10.1103/PhysRevB.85.180508>

This material is protected by copyright and other intellectual property rights, and duplication or sale of all or part of any of the repository collections is not permitted, except that material may be duplicated by you for your research use or educational purposes in electronic or print form. You must obtain permission for any other use. Electronic or print copies may not be offered, whether for sale or otherwise to anyone who is not an authorised user.

Fulde-Ferrell-Larkin-Ovchinnikov state in the dimensional crossover between one- and three-dimensional lattices

Dong-Hee Kim and Päivi Törmä*

Department of Applied Physics and Centre of Excellence in Computational Nanoscience (COMP), Aalto University, FI-00076 Aalto, Finland

(Received 12 December 2011; revised manuscript received 4 May 2012; published 24 May 2012)

We present a full phase diagram for the one-dimensional (1D) to three-dimensional (3D) crossover of the Fulde-Ferrell-Larkin-Ovchinnikov (FFLO) state in an attractive Hubbard model of 3D-coupled chains in a harmonic trap. We employ real-space dynamical mean-field theory which describes full local quantum fluctuations beyond the usual mean-field and local density approximation. We find strong dimensionality effects on the shell structure undergoing a crossover between distinctive quasi-1D and quasi-3D regimes. We predict an optimal regime for the FFLO state that is considerably extended to intermediate interchain couplings and polarizations, directly realizable with ultracold atomic gases. We find that the 1D-like FFLO feature is vulnerable to thermal fluctuations, while the FFLO state of mixed 1D-3D character can be stabilized at a higher temperature.

DOI: [10.1103/PhysRevB.85.180508](https://doi.org/10.1103/PhysRevB.85.180508)

PACS number(s): 67.85.-d, 74.25.N-, 03.75.Ss, 71.10.Fd

The interplay between fermion pairing and magnetism is at the heart of understanding strongly correlated systems ranging from unconventional superconductors and ultracold gases to neutron stars and quarks.¹ BCS-type superconductivity is suppressed by a large magnetic field exceeding the Chandrasekhar-Clogston limit. However, it has been proposed as a paradigm of superconductivity in high magnetic fields that it is possible for superconductivity and magnetism to coexist with exotic pairing mechanisms.²⁻⁵ The Fulde-Ferrell-Larkin-Ovchinnikov (FFLO) state would arise with this interplay,^{2,3} but it still remains elusive in spite of indirect experimental evidence observed.⁶ The FFLO state is characterized by the Cooper pair carrying finite momentum causing a spatially modulated order parameter. One peculiar feature of this exotic phase is that apparently its stability is largely affected by the dimensionality of the system. It turns out that the three-dimensional (3D)-FFLO state occupies a thin area of the mean-field phase diagram,⁷ though the signature can be stronger in systems that support nesting such as optical lattices^{8,9} and elongated traps.¹⁰ Indeed, only phase separation was observed for ultracold gases in 3D traps.¹¹⁻¹³ On the other hand, in the exact solution of a one-dimensional (1D) system, the FFLO character appears at any finite spin polarization,¹⁴ while long-range order cannot exist in 1D. The experiment¹⁵ in 1D was consistent with the FFLO theory, although the state remains unidentified.

A natural question arising is whether one can combine the promising 1D-FFLO features and long-range order provided by higher dimensions. This has been considered in previous mean-field¹⁶ and effective field theory¹⁷ studies for coupled continuum-1D gases, and for the Hubbard ladder.¹⁸ The trapping potential is essential in ultracold gas experiments, and thus in spin-polarized systems, one can expect a shell structure of different phases along the trap. Therefore, beyond the local density approximation, the inhomogeneous superfluid and normal phases need to be treated in a unified framework by including full local quantum fluctuations. Neglecting local quantum fluctuations creates an apparent bias in favor of the superfluid state and against the normal state.¹⁰ Here, using a real-space dynamical mean-field theory (DMFT), we investigate the 1D-3D crossover problem within the anisotropic Hubbard model in a trap.

The dimensionality effect to the FFLO state that we are considering here differs from the two-dimensional (2D)-3D crossover studied in layered superconductors.¹⁹ There, the quasi-2D character minimizes the orbital pair breaking effects in a magnetic field, and the Zeeman effect may then lead to a d -wave FFLO state. Here we consider s -wave pairing, and orbital effects are absent. Note that a particle-hole transformation can bring in another interesting perspective by mapping the FFLO state to the striped phase of the doped repulsive Hubbard model.²⁰ This emphasizes the importance of the FFLO state in the general context of high- T_c superconductivity.

We perform a real-space variant of DMFT calculations on the attractive Hubbard model of 3D-coupled chains,

$$\mathcal{H} = -t_{\parallel} \sum_{i\ell\sigma} (c_{i\ell\sigma}^{\dagger} c_{(i+1)\ell\sigma} + \text{H.c.}) - t_{\perp} \sum_{(l'l')} \sum_{i\sigma} c_{i\ell\sigma}^{\dagger} c_{i\ell'\sigma} + U \sum_{i\ell} \hat{n}_{i\ell\uparrow} \hat{n}_{i\ell\downarrow} + \sum_{i\ell\sigma} (V_i - \mu_{\sigma}) \hat{n}_{i\ell\sigma},$$

where $c_{i\ell\sigma}^{\dagger}$ ($c_{i\ell\sigma}$) creates (annihilates) a fermion with spin $\sigma = \uparrow, \downarrow$ at site i of chain ℓ , the density $\hat{n}_{i\ell\sigma} = c_{i\ell\sigma}^{\dagger} c_{i\ell\sigma}$. We define the superfluid order parameter as $\Delta = -\langle c_{\uparrow}^{\dagger} c_{\downarrow}^{\dagger} \rangle$. Throughout the calculations, the hopping t_{\parallel} is set to unity. The dimensionality is thus tuned by the interchain coupling t_{\perp} and varied from 1D ($t_{\perp} = 0$) to 3D ($t_{\perp} = 1$). The chemical potentials μ_{\uparrow} and μ_{\downarrow} control the polarization $P = (N_{\uparrow} - N_{\downarrow}) / (N_{\uparrow} + N_{\downarrow})$ by keeping the total particle number $N_{\uparrow} + N_{\downarrow} \sim 120$. The harmonic potential trapping the gases in a longitudinal chain is given as $V_i = 5 \times 10^{-5} (i - 1/2)^2$. The on-site interaction U is selected to be the value corresponding to unitarity where the 3D two-body scattering length diverges.²¹ The value of U varies from -2.038 ($t_{\perp} = 0.1$) to -7.915 ($t_{\perp} = 1$), which is comparable to the half bandwidths.

In order to treat an inhomogeneous phase along the chain, a site-dependent self-energy Σ_i is considered within DMFT.^{10,22,23} With translational invariance in transverse directions, the on-chain Green's function is written for sites i, j and transverse momentum \mathbf{k}_{\perp} as

$$[\mathbf{G}^{-1}(\mathbf{k}_{\perp}; i\omega_n)]_{ij} = [i\omega_n \boldsymbol{\sigma}_0 - \epsilon_{\mathbf{k}_{\perp}} \boldsymbol{\sigma}_3 - \Sigma_i(i\omega_n)] \delta_{ij} - \mathbf{h}_{ij}^{\parallel},$$

where ω_n denotes the Matsubara frequency, σ is the Pauli matrix, \mathbf{h}^{\parallel} is the noninteracting part of the chain Hamiltonian, the 2D energy dispersion $\epsilon_{\mathbf{k}_{\perp}} \equiv -2t_{\perp}(\cos k_x + \cos k_y)$ with $\mathbf{k}_{\perp} = (k_x, k_y)$, and the operators are in the Nambu basis. In the self-consistency of DMFT, the impurity Green's function is obtained as $\mathcal{G}_i(i\omega_n) = \sum_{\mathbf{k}_{\perp}} \mathcal{G}_{ii}(\mathbf{k}_{\perp}; i\omega_n)$. While we have a local but site-dependent self-energy term, the procedures can be compared to the chain-DMFT.²⁴ The exact diagonalization method is employed to solve the site-dependent impurity problem.¹⁰

With the on-site interaction $U = -4$, we have found that our calculations qualitatively reproduce the two important characteristics of strongly interacting 1D Fermi gases.^{14,25} First, at small polarizations, the trap edges are fully paired while the trap center is partially polarized. The entire area becomes polarized as the total polarization increases. Second, at finite polarizations, the polarized trap center is associated with the FFLO state exhibiting a spatially oscillating order parameter.

Clear features of getting away from the 1D limit are observed. For the studied finite interchain couplings, the pairing at the edges, namely, the first 1D feature listed above, is easily broken at small polarizations. This indicates that immediately away from 1D, one can observe fully polarized edges much before the whole area gets polarized. In contrast, it turns out that the other part of the 1D features, the emergence of a partially polarized center in fully paired vicinities, survives at small interchain couplings. Away from but close to the 1D limit, we typically find a shell structure of polarized edges, fully paired shoulders, and a partially polarized center.

In Fig. 1, we present a real-space DMFT phase diagram of the Hubbard model of 3D-coupled chains at zero temperature. Considering only the phase at the trap center, we find that the emergence of the FFLO-type oscillating order parameter occupies a large area of polarizations and interchain couplings. This wide coexistence area of a finite density difference and a finite order parameter extends all the way to the 3D limit, as opposed to the mean-field phase diagram on a 3D continuum where the FFLO phase occupies only a tiny area.⁷

Our zero-temperature phase diagram characterizes the emergence of three types of shell structures, as shown in Fig. 1(b). First, area I shows quasi-3D features in the shell structure where the fully paired superfluid (SF) core exists. There are FFLO-type oscillations found between the SF core and the fully polarized edges. Second, area II shows an inverted sequence: an FFLO core surrounded by fully paired shoulders. The edges are polarized in this area, and small order parameter oscillations also exist at the interfaces between the fully paired shoulders and the fully polarized edges. While this indicates a mixture of 1D and 3D features, area II can be identified as a quasi-1D phase because of the spatial pattern of the FFLO oscillations emerging at the trap center. Area II is only found at interchain couplings $t_{\perp} \leq 0.3$. Third, area III has a two-shell structure where the FFLO-type oscillations reside in the entire area of the partially polarized core, surrounded by fully polarized edges. Area III is found across the whole range of interchain couplings at intermediate-high polarizations below the transition to the normal phase.

We find that the FFLO character evolves very differently with polarization in the quasi-1D and quasi-3D regimes.

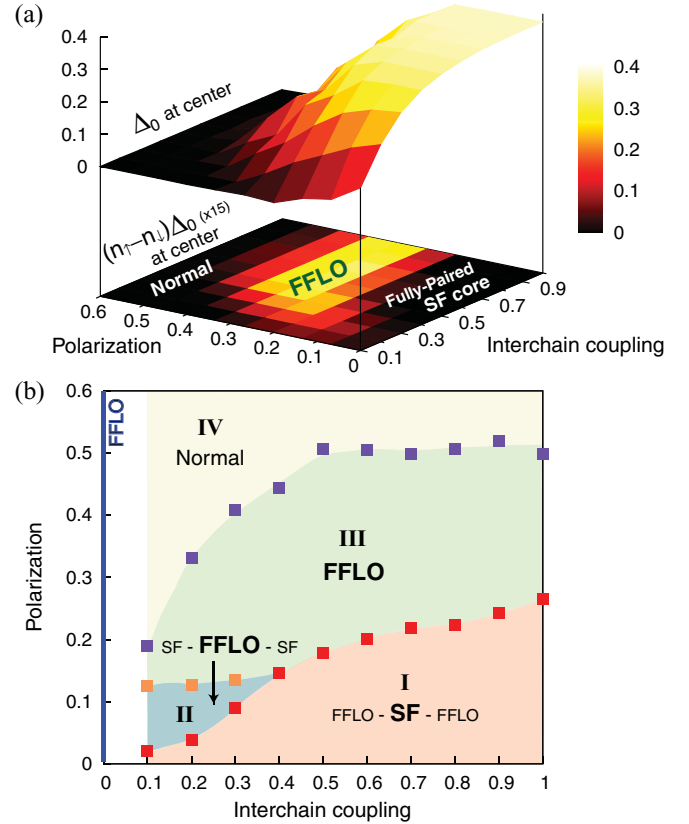


FIG. 1. (Color online) Phase diagram of the 3D coupled-chain Hubbard model. The particle densities $n_{\uparrow,\downarrow}$ and the order parameter Δ are calculated as a function of the interchain coupling and the polarization at zero temperature. (a) The oscillation amplitude Δ_0 of the order parameter and the density difference $n_{\uparrow} - n_{\downarrow}$ at the trap center. The phases at the trap center can be divided into three: the fully paired superfluid (SF) ($n_{\uparrow} = n_{\downarrow}, \Delta \neq 0$), FFLO (oscillating n and Δ), and normal ($\Delta = 0$) phases. (b) Phases I–III associated with the shell structures in the trap, explained in the text.

Figure 2 shows the shell structures with increasing polarization P at both sides of the 1D-3D crossover. In the quasi-1D regime [Fig. 2(a)], the evolution is dominated by the expansion of the FFLO core. In contrast, in the quasi-3D regime [Fig. 2(b)], the fully paired core shrinks with increasing P while the FFLO-type oscillations at the shoulders move toward the trap center. Near the crossover, these quasi-1D and quasi-3D features coexist. At the interchain coupling $t_{\perp} = 0.3$, the oscillations of the order parameter Δ become significant at both the trap center and edges, and the fully paired shoulders decrease from both sides as P increases. In addition, when P is increased to enter area III, the oscillations of Δ along the trap show a distinct feature: At small t_{\perp} , the amplitude of Δ becomes spatially uniform, despite the trap, at intermediate P [see Fig. 2(c)]. This can be compared to the zero derivative of the FFLO momentum as a function of the chemical potential.¹⁶ The uniform oscillations occur only in the quasi-1D regime, raising the possibility that a peak signal of the FFLO momentum is more visible in this regime.

Our phase diagram suggests that the optimum spot for observing the FFLO state is extended over a significantly large area of the dimensional crossover. In particular, the largest

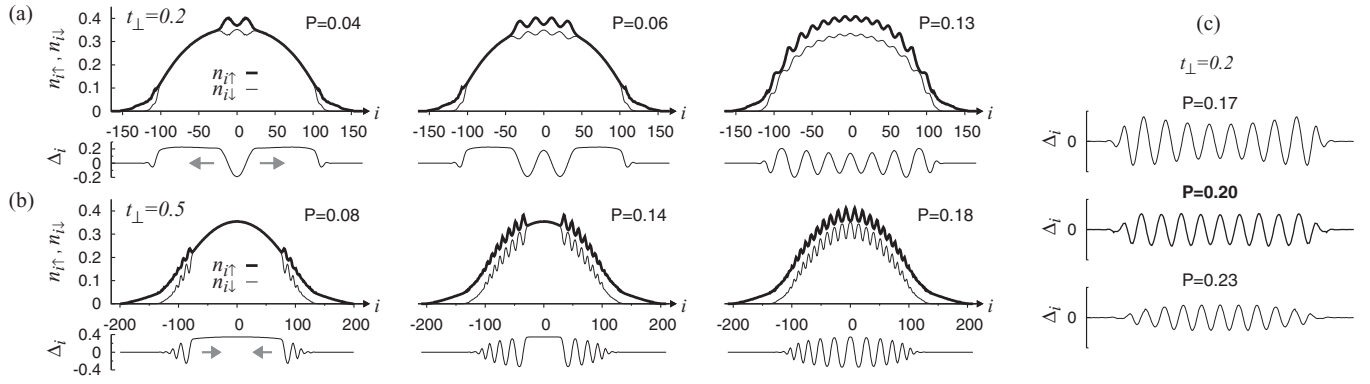


FIG. 2. Evolution of the FFLO oscillations in the 1D-3D crossover. The profiles of the particle densities $n_{\uparrow,\downarrow}$ and the order parameter Δ along the chain sites i are presented for the two regimes of interchain couplings (a) $t_{\perp} = 0.2$ (quasi-1D) and (b) $t_{\perp} = 0.5$ (quasi-3D). In the quasi-1D regime, for small polarization $P = 0.04$, the FFLO-type oscillations at the center are surrounded by the fully paired shoulders. The region of oscillating Δ develops from the center, expands toward the edges as P increases, and then emerges over the whole area for $P = 0.13$. On the contrary, in the quasi-3D regime, the oscillations are initially at the partially polarized intermediate regions and spread toward the center as P increases. At finite interchain couplings, the far edges of the trap are always polarized. In (c), the evolution of the oscillation envelope of Δ is shown with increasing P at $t_{\perp} = 0.2$ in the quasi-1D regime. Uniform oscillations occur along the trap at an intermediate polarization.

range of polarizations associated with the FFLO-featured areas (II + III) at the trap center is found around interchain coupling $t_{\perp} \sim 0.4$. Since we still have two control parameters, the on-site interaction and the temperature, the phase diagram should be further generalized to discuss ultracold gas experiments which are conducted at finite temperatures and with a tunable atomic scattering length. We have examined also a stronger interaction $U = -4$ at small t_{\perp} 's, including the 1D limit ($t_{\perp} = 0$) where the 3D scattering approach fails. At small interchain couplings, we have found that the main effect of a stronger interaction is to increase the critical polarization of the transition to the normal phase while the change in the phase II area is relatively small. In the 3D limit, stronger interactions tend to keep the fully paired SF core even at larger polarizations, as observed in the previous experiments in the BEC regime,¹¹ which can make the 3D-FFLO area much smaller.

The stability of the FFLO state at finite temperature is a crucial question. We have examined the behavior at a finite temperature $T = 0.05$ near the dimensional crossover at the interchain coupling $t_{\perp} = 0.3$. A low temperature algorithm is used.²⁶ We find that a finite temperature can stabilize the polarized superfluid (pSF) state at small polarizations while it destroys the quasi-1D FFLO character. Figure 3 shows comparisons between the density and order parameter profiles at two different temperatures $T = 0.05$ and $T = 0$. These profiles indicate that area II with the FFLO core melts at $T = 0.05$ into the pSF state, similar to the results in 1D.²⁷ In the case of shell structures, the polarization from the FFLO area is easily redistributed in the trap at finite temperature to create a BCS-type order parameter with extra majority particles accommodated as thermal quasiparticles. In contrast, it turns out that area III with a trap-wide FFLO character at higher polarizations is not affected by the finite temperature examined.

A comparison with the previous mean-field results in 1D and 3D lattices shows the drastic effects of local quantum fluctuations: (1) Our results indicate that the large size of the FFLO area predicted by mean-field theory in 3D lattices^{8,9}

may have been overestimated. In the 3D limit, we find that the FFLO state is broken near local polarization 0.35 at a trap center that is approximately a quarter filled, which contrasts to the mean-field values ~ 0.6 ($|U| = 5.14$)⁸ and ~ 0.75 ($|U| = 6$)⁹ at the same filling. This enhancement of the normal state can be understood in light of the fact that including the particle-hole channel was shown to reduce pairing significantly in lattices:²⁸ DMFT includes full local quantum fluctuations, causing such higher order effects. (2) In 1D lattices, mean-field theory²⁹ predicted only a 3D-like shell structure with a fully paired center and polarized edges.

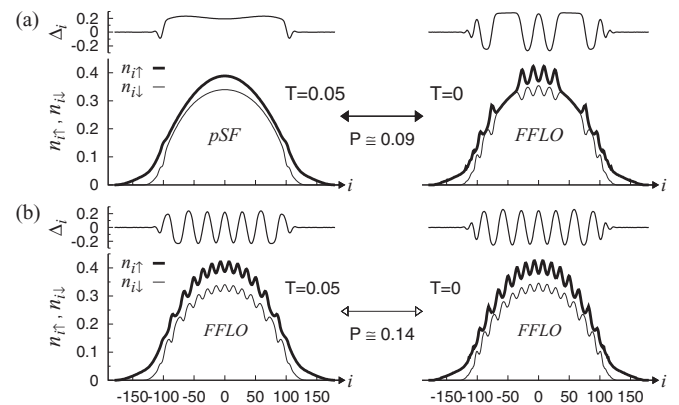


FIG. 3. Polarized superfluid phase at finite temperature. For interchain coupling $t_{\perp} = 0.3$, the profiles at temperature $T = 0.05$ are compared with those at $T = 0$ for the particle densities $n_{\uparrow,\downarrow}$ and the order parameter Δ along the chain sites i . At polarization (a) $P \simeq 0.09$, corresponding to phase II, the structure of the FFLO core surrounded by fully paired shoulders found at $T = 0$ is completely changed into the polarized superfluid phase with a uniform order parameter at $T = 0.05$. The order parameter oscillations at the edges are still observed at $T = 0.05$. In contrast, at a higher polarization (b) $P \simeq 0.14$, corresponding to phase III, similar FFLO characteristics are identified at both temperatures $T = 0.05$ and $T = 0$.

In contrast, we find the reversal of the shell structure, similar to what has been predicted by continuum mean-field study.¹⁶ (3) In addition, our characterization of the FFLO state does not find the well-separated domain wall between the sign changes of the order parameter predicted by the mean-field theories in lattices⁹ and in continuum.¹⁶ Our findings, the drastic decrease of critical polarization, the shell structure reversal, and the absence of domain walls, emphasize the importance of local quantum fluctuations in lattices, regardless of the dimensionality.

Our findings are directly applicable to future experiments. Recent experiments realized a weakly coupled 2D array of 1D tubes with ultracold ⁶Li gases, observing the density profile characteristics of attractively interacting spin-polarized 1D Fermi gases.¹⁵ This system can be further extended toward the quasi-1D regime by adjusting the optical lattice potentials, and, if needed, discreteness along the tube direction can be realized by 3D lattices.^{30,31} Although it is nontrivial to experimentally reveal the oscillating order parameter, several methods have been recently suggested to detect the FFLO state, particularly in 1D systems—see Refs. 32 and 33 and references therein.

Our DMFT calculations have shown that the FFLO phase occupies a significant area of the phase diagram throughout the 1D-3D crossover. In addition, our calculations at finite temperature have found that the FFLO character is more stable at intermediate rather than small polarizations where the phase becomes the polarized superfluid at low temperature. Our findings will help identify the presence of the FFLO state in ultracold atomic gases. In a general perspective, by using beyond-mean-field calculations we have investigated the dimensionality effects on the existence of the FFLO state in 1D-3D lattice systems. This may potentially help to understand also the puzzling repulsive Hubbard model counterparts such as the striped phase.

This work was supported by the Academy of Finland through its Centers of Excellence Programme (2012-2017) and under Projects No. 139514, No. 141039, No. 213362, and No. 135000 and conducted as a part of a EURYI scheme grant (see www.esf.org/euryi). Computing resources were provided by CSC—the Finnish IT Centre for Science and the Triton cluster at Aalto University.

*paivi.torma@aalto.fi

¹R. Casalbuoni and G. Nardulli, *Rev. Mod. Phys.* **76**, 263 (2004).

²P. Fulde and R. A. Ferrell, *Phys. Rev.* **135**, A550 (1964).

³A. I. Larkin and Y. N. Ovchinnikov, *Zh. Eksp. Teor. Fiz.* **47**, 1136 (1964) [*Sov. Phys. JETP* **20**, 762 (1965)].

⁴G. Sarma, *J. Phys. Chem. Solids* **24**, 1029 (1963).

⁵W. V. Liu and F. Wilczek, *Phys. Rev. Lett.* **90**, 047002 (2003).

⁶H. A. Radovan, N. A. Fortune, T. P. Murphy, S. T. Hannahs, E. C. Palm, S. W. Tozer, and D. Hall, *Nature (London)* **425**, 51 (2003).

⁷D. E. Sheehy and L. Radzihovsky, *Phys. Rev. Lett.* **96**, 060401 (2006).

⁸T. K. Koponen, T. Paananen, J.-P. Martikainen, and P. Törmä, *Phys. Rev. Lett.* **99**, 120403 (2007).

⁹Y. L. Loh and N. Trivedi, *Phys. Rev. Lett.* **104**, 165302 (2010).

¹⁰D.-H. Kim, J. J. Kinnunen, J.-P. Martikainen, and P. Törmä, *Phys. Rev. Lett.* **106**, 095301 (2011).

¹¹M. W. Zwierlein, A. Schirotzek, C. H. Schunck, and W. Ketterle, *Science* **311**, 492 (2006).

¹²G. B. Partridge, W. Li, R. I. Kamar, Y. Liao, and R. G. Hulet, *Science* **311**, 503 (2006).

¹³S. Nascimbène, N. Navon, K. J. Jiang, L. Tarruell, M. Teichmann, J. McKeever, F. Chevy, and C. Salomon, *Phys. Rev. Lett.* **103**, 170402 (2009).

¹⁴K. Yang, *Phys. Rev. B* **63**, 140511(R) (2001).

¹⁵Y. Liao, A. S. C. Rittner, T. Paprotta, W. Li, G. B. Partridge, R. G. Hulet, S. K. Baur, and E. J. Mueller, *Nature (London)* **467**, 567 (2010).

¹⁶M. M. Parish, S. K. Baur, E. J. Mueller, and D. A. Huse, *Phys. Rev. Lett.* **99**, 250403 (2007).

¹⁷E. Zhao and W. V. Liu, *Phys. Rev. A* **78**, 063605 (2008).

¹⁸A. E. Feiguin and F. Heidrich-Meisner, *Phys. Rev. Lett.* **102**, 076403 (2009).

¹⁹Y. Matsuda and H. Shimahara, *J. Phys. Soc. Jpn.* **76**, 051005 (2007).

²⁰A. Moreo and D. J. Scalapino, *Phys. Rev. Lett.* **98**, 216402 (2007).

²¹E. Burovski, N. Prokof'ev, B. Svistunov, and M. Troyer, *Phys. Rev. Lett.* **96**, 160402 (2006).

²²A. Georges, G. Kotliar, W. Krauth, and M. J. Rozenberg, *Rev. Mod. Phys.* **68**, 13 (1996).

²³M. Snoek, I. Titvinidze, and W. Hofstetter, *Phys. Rev. B* **83**, 054419 (2011).

²⁴S. Biermann, A. Georges, A. Lichtenstein, and T. Giamarchi, *Phys. Rev. Lett.* **87**, 276405 (2001).

²⁵G. Orso, *Phys. Rev. Lett.* **98**, 070402 (2007).

²⁶M. Capone, L. de' Medici, and A. Georges, *Phys. Rev. B* **76**, 245116 (2007).

²⁷M. J. Wolak, V. G. Rousseau, C. Miniatura, B. Grémaud, R. T. Scalettar, and G. G. Batrouni, *Phys. Rev. A* **82**, 013614 (2010).

²⁸D.-H. Kim, P. Törmä, and J.-P. Martikainen, *Phys. Rev. Lett.* **102**, 245301 (2009).

²⁹T. K. Koponen, T. Paananen, J.-P. Martikainen, M. R. Bakhtiari, and P. Törmä, *New J. Phys.* **10**, 045014 (2008).

³⁰R. Jördens, N. Strohmaier, K. Günter, H. Moritz, and T. Esslinger, *Nature (London)* **455**, 204 (2008).

³¹U. Schneider, L. Hackermüller, S. Will, Th. Best, I. Bloch, T. A. Costi, R. W. Helmes, D. Rasch, and A. Rosch, *Science* **322**, 1520 (2008).

³²J. M. Edge and N. R. Cooper, *Phys. Rev. Lett.* **103**, 065301 (2009).

³³J. Kajala, F. Massel, and P. Törmä, *Phys. Rev. A* **84**, 041601(R) (2011).